Polarization and Angular Dependence of 1.06-μm Laser-Light Absorption by Planar Plasmas

K. R. Manes, V. C. Rupert, J. M. Auerbach, P. Lee, and J. E. Swain
Lawrence Livermore Laboratory, University of California, Livermore, California 94550
(Received 13 May 1977)

An enclosing "box" calorimeter has been used to measure the polarization and angular dependence of 1.06-μm laser-light absorption under experimental conditions approximating those assumed by Estabrook, Valeo, and Kruer in their simulations; i.e., $\sim 10^{16}$ W/cm^2 plane waves incident on a planar plasma. A clear resonance absorption maximum was observed for p- but not for s-polarized incident radiation as predicted.

The production of laser-heated inertially confined thermonuclear plasmas involves several stages. Foremost among these is the coupling of laser energy into the target plasma; therefore, the nature of this laser-light absorption process has been the subject of much theoretical and experimental research.[1-11] Estabrook, Valeo, and Kruer have carried out two-dimensional relativistic simulations of plasma absorption.[1] Their calculations show a maximum absorption efficiency of approximately 50%, generation of suprathermal particles, and strong steepening of the density profile in the vicinity of the critical density. The dominant mechanism in these calculations is resonance absorption which, in this context, refers to a collisionless plasma-heating mechanism arising for obliquely incident radiation. If the radiation's electric-field vector has a component along the density gradient direction, electron plasma waves may be excited, leading to plasma heating.

Recently a body of experimental evidence has accumulated which supports the proposition that an important process governing the absorption of laser pulses less than ~100 ps in duration with intensities between $\sim 10^{14}$ and $\sim 10^{16}$ W/cm^2 is resonance absorption.[4-11] Here we report the results of an experimental attempt to observe the polarization and angular dependence of the absorption of 1.06-μm optical plane waves incident on flat slabs; i.e., conditions similar to those used in the simulations of Estabrook, Valeo, and Kruer. Direct experimental evidence of resonance absorption has been produced using the Janus laser facility.

The experimental design employed for these measurements is indicated schematically in Fig. 1. The ~100-GW 1.06-μm laser pulses (30 ± 6 ps in duration) were provided by one beam of the Janus laser/target interaction facility.[12] The Janus oscillator-amplifier laser system is routinely capable of delivering ~400 GW in two beams to laser fusion targets; however, for this study Janus was limited to $\lesssim$100-GW single-beam irradiations in order to avoid the complications which nonlinear intensity-dependent phase distortions might have introduced.[13] The laser pulses were focused onto the ~300-μm-diam, ~20-μm-thick parylene (C_8H_8) disk targets by an aspheric $f/10$ lens. The input-beam profile at the $f/10$ lens was approximately rectangular ("top-hat" beam); thus the diffraction-limited focal-spot diameter should have been ~26 μm. In practice, the full aperture of the lens was not used and astigmatism ≤ 1 wave was observed in the beam. A typical target and target-plane intensity distribution are

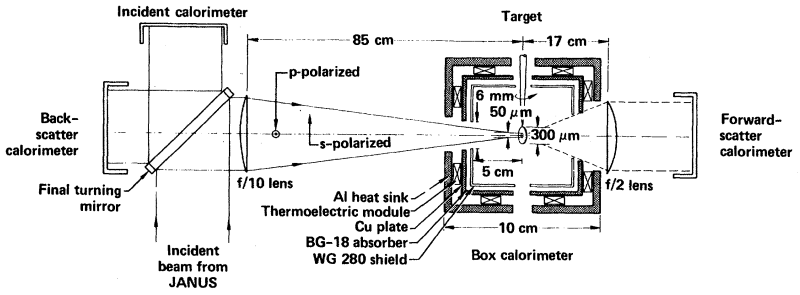

FIG. 1. Approximately 100-GW pulses from Janus were focused through a small opening in the box calorimeter on to the rotatable targets. Scattered 1.06-μm light not accounted for by forward- and back-scatter calorimeters was transmitted by the WG280 shield and absorbed by the BG-18 glass. The subsequent temperature rise of the BG-18 glass and Cu plate assembly was monitored by thermoelectric modules.

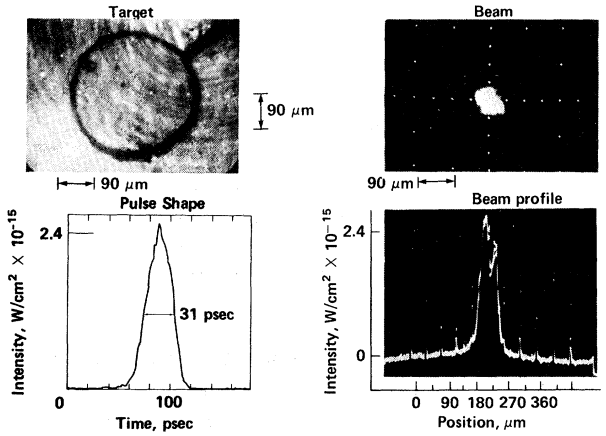

FIG. 2. Typical target, target-plane intensity distribution and temporal pulse shape. A scan through the beam image provided the profile below, and a streak camera located at the laser-system output measured the temporal shape of the pulse reaching the target on every shot.

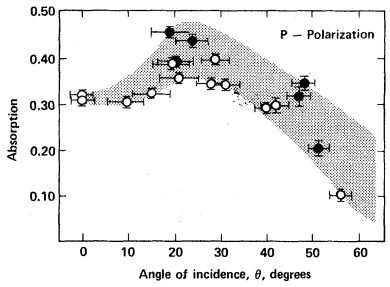

FIG. 3. The measured absorption of p-polarized light is plotted vs the angle θ between the target normal and the incident-beam k vector. The shaded region indicates the extremes of the data and the error bars indicate relative errors; however, the calorimeters were absolutely calibrated to $\leq \pm 5\%$. Dots and circles indicate intensity range: ●, $(5.6 \pm 0.4) \times 10^{15}$ W/cm^2; ○, $(2.5 \pm 0.9) \times 10^{15}$ W/cm^2.

shown in Fig. 2. This intensity distribution was recorded on every target shot and varied slowly due to laser disk heating and minor misalignment; however, the focal-spot diameter at the target was always within the range 40 ± 17 μm.[4] Each target was prealigned using a microscope such that the orientation of its normal with respect to the target manipulator was known. After insertion into the target chamber, the target was illumited by diffused 1.06-μm light through the $f/2$ lens. The target manipulator was then rotated through the desired angle, θ. Because the laser spot in the target plane was observed by the same $f/2$ lens, it could be located to within ± 5 μm of the center of each transparent target. The Rayleigh range calculated for this $f/10$ focusing geometry is between 200 and 500 μm, and as expected, the laser-spot area changed only slightly for a several-hundred-micron axial translation of the $f/10$ lens.

Laser pulse duration was determined on every target shot by an optical streak camera located at the laser output. A typical temporal pulse shape is displayed in Fig. 2. Because the plasma expansion velocity has been measured to be $(3 \pm 1) \times 10^7$ cm/sec, the plasma front moves only 12 μm during the laser pulse. In summary, the target was presented with an almost planar wave front and the pulse duration was short enough to preserve the angle between the laser beam and the target normal to reasonable accuracy. The intensity range realized in this experiment, 10^{15} to 10^{16} W/cm^2, was chosen to be within the range of Estabrook, Valeo, and Kruer's simulations, relevant to spherical-target work and high enough to minimize classical collisional (inverse bremsstrahlung) absorption.

After striking the target, the scattered laser light was collected by an enclosing box calorimeter indicated in Fig. 1.[4,9,14] The 1.06-μm radiation was transmitted by the WG280 glass shield and absorbed by the BG-18 glass. Since ions, electrons, and all but the most energetic x rays (≥ 15 keV) were stopped by the shield, this calorimeter provided an accurate measure of scattered light. Light reflected back into the focusing-lens cone was measured by a backscatter calorimeter and, similarly, forward-scattered radiation was directed into another calorimeter. Each of these calorimeters was calibrated *in situ* and corrected for extraneous effects such as stray flashlamp light since the experiment required better than 1% accuracy from each detector. Recalibrations of the laser calorimeters were performed after each configuration change; i.e., prior to p-polarization shots, upon changing to s polarization, and when a return to p polarization was made to check several points at the end of the experiment. In addition, the transmissions and reflections of all optical elements were measured in place for each polarization. Finally, the polarization of the incident laser light was measured by polarimetry of the pulsed beam and was adjusted to within one degree of the desired state.

Figures 3 and 4 show the measured absorptions for p- and s-polarized light, respectively. The absorption measured at normal incidence should

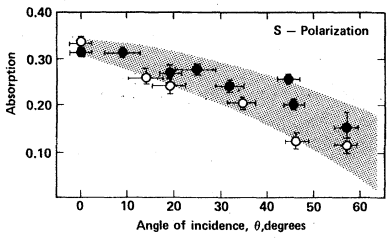

FIG. 4. The absorption of s-polarized light declines monotonicly with increasing θ. The shaded region indicates the extremes of the data and dots and circles indicate intensity range: ●, $(8.5\pm4.0)\times10^{15}$ W/cm^2; ○, $(2.6\pm0.4)\times10^{15}$ W/cm^2.

be the same for both polarizations, and indeed it is the same, within measurement accuracy. For s-polarized radiation, the absorption decreases monotonically with angle of incidence. For p-polarized light, a maximum occurs between $\theta = 20°$ and 25°. The data points fell into two target-surface–intensity groups as indicated in Figs. 3 and 4. The shaded regions indicate the approximate extremes of our measurement, and the higher values of absorption at each angular setting correspond to higher intensity at the target surface. This intensity effect is particularly evident in the s-polarized–light absorption measurements and probably accounts for the elevated p-polarized–light absorptions observed at 20° and 50°. Even with the range of intensities and absorptions encountered on different trails, the resonance for p-polarized light is clearly evident while no similar maximum was observed in the s-polarized–light measurements.

The angle corresponding to the absorption maximum for p polarization coupled with Ginzburg's resonance absorption function[15] implies a scale length of

$$L = \left(\frac{0.8}{\sin\theta}\right)^3 \frac{c}{\omega} \cong 1\text{–}2\ \mu\text{m},$$

in agreement with previous results obtain by polarimetry.[10]

A seven-channel x-ray spectrometer was used to measure the continuum thermal x-ray "temperature" on several shots.[16] Typical temperatures obtained were of the order of 600 eV. By assuming a linear ramp electron-density profile with a scale height of 1 to 2 μm, an estimate for the classical collisional absorption may be made:

$$A \cong 1 - \exp\left[\tfrac{32}{15}(\nu L/c)\cos^5\theta\right] \leq 0.08,$$

where ν is the electron-ion collision frequency. Hence at $\theta = 0°$ a substantial (>20%) absorption due to anomalous or nonlinear effects was observed, which is more than that predicted by the simulations in Ref. 1.

Quantitative differences between the calculated and measured p-polarized–light absorption may be due partly to the departure of the experiment from the ideal-illumination configuration assumed in the calculations. Indeed, the incident radiation was not perfectly collimated and the targets were not identical or perfectly flat. Electron-density–profile rippling or cavity formation may account for some of the discrepancies.[17] Other mechanisms which might modify the absorption and smooth its angle and polarization dependence include short wavelength ion turbulence,[18] resonance absorption due to self-generated magnetic fields,[19] and the $2\omega_{pe}$ instability.[20]

The fraction of the incident energy backscattered into the $f/10$ focusing lens reached a maximum of 2% for $\theta = 0°$, but for all other angles investigated was 1% or less. This small percentage of directly backscattered radiation suggests a diffuse scattering surface and may present indirect experimental evidence of cratering; however, the initial roughness of the target face could have the same effect. In any case, this low backscatter suggests that stimulated back-reflection was not significant in this measurement.

In summary, a clear maximum in the p-polarized–laser–light absorption by parylene targets has been observed at angles of incidence between 20° and 25° in qualitative agreement with theory.[1] The s-polairzed–light measurements exhibit a monotonic decrease of the absorption with the angle of incidence. This clear signature of the resonance absorption phenomenon observed at intensities and pulse durations typical of exploding-pusher laser fusion studies, identifies resonance absorption as a significant absorption mechanism for this class of experiments.

The authors wish to acknowledge the contributions of their colleagues, H. G. Ahlstrom, J. H. Nuckolls, W. L. Kruer, C. E. Max, W. Mead, J. J. Thomson, E. Storm, C. Hendricks, W. Radke, R. Bolt, K. Andrus, and T. Schwinn. This work was performed under the auspices of the U. S. Energy Research and Development Administration under Contract No. W-7405-Eng-48.

[1]K. G. Estabrook, E. J. Valeo, and W. L. Kruer, Phys. Fluids 18, 1151 (1975).

[2]J. P. Freidberg, R. W. Mitchell, R. L. Morse, and

L. I. Rudsinski, Phys. Rev. Lett. 28, 795 (1972); D. W. Forslund, J. M. Kindel, Kenneth Lee, E. L. Lindman, and R. L. Morse, Phys. Rev. A 11, 679 (1975).

[3]B. Ripin *et al.*, Phys. Rev. Lett. 34, 1313 (1975); E. Fabre and C. Stenz, Phys. Rev. Lett. 32, 823 (1974); C. Yamanaka, T. Yamanaka, T. Sasaki, and J. Mizui, Phys. Rev. Lett. 32, 1038 (1974); B. Ripin, Appl. Phys. Lett. 30, 134 (1977).

[4]K. R. Manes, H. G. Ahlstrom, R. A. Haas, and J. F. Holzrichter, Lawrence Livermore Laboratory Report No. UCRL-78771 (to be published).

[5]J. S. Pearlman, J. J. Thomson, and C. E. Max, Phys. Rev. Lett. 38, 1397 (1977).-

[6]P. Kolodner and E. Yablonovitch, Phys. Rev. Lett. 37, 1754 (1976).

[7]W. Mead *et al.*, Phys. Rev. Lett. 37, 489 (1976).

[8]W. Kruer, R. Haas, W. Mead, D. Phillion, and V. Rupert, in *Plasma Physics: Nonlinear Theory and Experiments*, edited by H. Wilhelmsson (Plenum, New York, 1977), pp. 64–81.

[9]R. A. Haas *et al.*, Phys. Fluids 20, 322 (1977).

[10]D. W. Phillion *et al.*, Lawrence Livermore Laboratory Report No. UCRL-78444 (to be published).

[11]E. K. Storm *et al.*, Lawrence Livermore Laboratory Report No. UCRL-79030 (to be published).

[12]D. R. Speck and F. Rienecker, Lawrence Livermore Laboratory Report No. UCRL 50021-74, 1974 (unpublished), p. 35.

[13]J. A. Glaze, Opt. Eng. 15, 136 (1976).

[14]S. R. Gunn, unpublished; S. R. Gunn and V. C. Rupert, to be published.

[15]V. L. Ginsburg, *The Propagation of Electro-magnetic Waves in Plasmas* (Pergamon, New York, 1969).

[16]V. W. Slivinsky, H. N. Kornblum, and H. D. Shay, J. Appl. Phys. 46, 1973 (1975).

[17]K. G. Estabrook and E. J. Valeo, Lawrence Livermore Laboratory Report No. UCRL 77146, 1975 (unpublished); J. J. Thomson and C. Randall, private communication.

[18]R. J. Faehl and W. L. Kruer, Phys. Fluids 20, 55 (1977); W. Manheimer, Phys. Fluids 20, 265 (1977).

[19]W. L. Kruer and K. G. Estabrook, in *Laser Interaction and Related Plasma Phenomena*, edited by H. Schwarz and H. Hora (Plenum, New York, to be published), Vol. 4.

[20]A. B. Langdon and B. F. Lasinski, in *Methods in Computational Physics*, edited by J. Killeen *et al.* (Academic, New York, 1976), Vol. 16.

Theory of Hot-Electron Spectra at High Laser Intensity

D. W. Forslund, J. M. Kindel, and K. Lee

Theoretical Division, Los Alamos Scientific Laboratory, Los Alamos, New Mexico 87545

(Received 17 January 1977)

A simple model involving resonant absorption in a self-consistent sharp density gradient is found to be in quantitative agreement with the suprathermal-electron spectrum from recent laser-plasma–interaction experiments and to explain qualitatively the scaling of that suprathermal-electron spectrum with laser power and wavelength.

There has been considerable controversy in recent years on the source of the hot or suprathermal electrons and high-energy x rays observed in high-powered–laser–target experiments.[1-5] We propose in this Letter a simple model which quantitatively agrees with experimental data from a variety of laboratories. In particular, we present an explanation as to why the hot-electron temperature in laser-produced plasmas at high incident laser intensity scales weakly with both laser wavelength and laser intensity. We find that at high laser power the self-consistent steepening of the plasma density profile in which the laser penetrates to densities greatly exceeding the critical density results in resonant absorption being the dominant absorption mechanism. At the same time the electron-heating mechanism of resonant absorption allows the steepened profile to persist. In this quasiequilibrium state this model predicts that the characteristic hot-electron energy, T_H, is given approximately (in keV) by

$$T_H \sim 14(I\lambda^2)^{1/3}T_c^{1/3}, \quad (1)$$

where I is the laser intensity in units of 10^{16} W/cm^2, λ is the laser wavelength in micrometers, and T_c is the background electron temperature in keV at the critical density.

At one point hot-electron temperatures were thought to scale as $I\lambda^2$ on the basis of infinite-homogeneous-plasma simulations or heat-capacity arguments.[6] Flux-limit arguments in which the bulk of the electrons are stochastically heated in a region around the critical density predict[7] that the electron temperature scales as $(I\lambda^2)^{2/3}$. In addition, the argument that the energy is car-

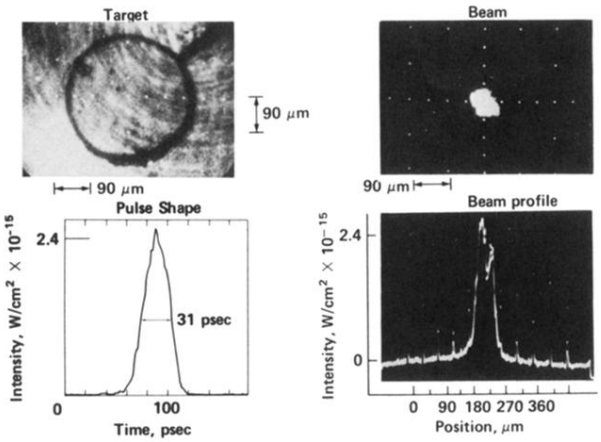

FIG. 2. Typical target, target-plane intensity distribution and temporal pulse shape. A scan through the beam image provided the profile below, and a streak camera located at the laser-system output measured the temporal shape of the pulse reaching the target on every shot.